Tribological Behaviour of Stellite Matrix Composites For High Temperatures Applications

DELBÉ Karl[1,a], OROZCO GOMEZ Solisabel[1],
CARRILLO MANCUSO Juan Manuel[1], PARIS Jean-Yves[1], DENAPEJean[1]

[1] LGP, ENIT-INPT, Université de Toulouse, 47, avenue d'Azereix, BP 1629 - 65016 -TARBES CEDEX
[a] Karl.Delbe@enit.fr

Keywords: Tribology, wear, metal matrix composites, solid lubricants.

Abstract. Extreme working conditions affect material used as friction components in transportation field: they rapidly reach their limits and critical parts require to be regularly replaced. Alternative solutions withstanding higher operating conditions imply to find innovative materials. Stellite matrix composites including various solid lubricants, WS_2 and h-BN, able to admitextreme conditions were developed using a Spark Plasma Sintering technique, which makes possible the formation of new microstructures out of reach by conventional means. Sliding tests were conducted using a pin-on-disc tribometer in air at 450°C, with a velocity of 0,25 m/s and various normal load ranged from 2.5 to 40 N. Influence of solid lubricant content and sensitivity to test parameters were studied in terms of friction and wear responses of the contacting materials. Friction properties are equivalent to Stellite ones and sometimes lesseffective. A reduction of wear is quantified for many composites, and the best behavior is observed for those that contain WS_2. In agreement with the third body approach, interpretations are proposed to describe the interphase dynamics within the contact.

Introduction

In current industry, mechanical devices assume to supportsevere environmental conditions: high temperature and stresses under reactive and corrosive conditions. Economic pressures and new environmental standards require manufacturers to find innovative solutions for the replacement of out-of-date parts.

Insertion of a solid lubricant in a composite material in order to reduce friction and wearhas already been considered widely by using conventional sintering method [1,2, 3, 4].Some studies have shown that the addition of solid lubricant can change the tribological properties of a metal matrix composite. Bolton and Gant acted on steel by adding particles of titanium carbide and niobium as well as two solid lubricants such as manganese sulfide and calcium fluoride [5].More recently, B. Chen and collaborators hadmade composites of copper and were added to graphite or hexagonal boron nitride in different proportions. The tribological test results showed that significantly improved the graphite friction reducing properties of the base and the boron nitride was not as effective [6]. W. Chen realized in 2010 a similar approach on ceramic composites SiN_4 type with hexagonal boron nitride. This combination was effective in tribological tests carried out with a steel punch [7].

Metal Matrix Composites (MMC) manufactured by Spark Plasma Sintering (SPS) provide original solutions for the synthesis of new materials inaccessible by conventional techniques.Thus,MMC containing different contents of solid lubricants such as hexagonal boron nitride (h-BN) or tungsten disulphide (WS_2) were worked out [1,8]. The presence of solid lubricant in the composite bulk and, in particular, on it surface,expects the formation of a tribofilm, so called third body, which will allow thevelocitiesaccommodation between surfaces in contact [9,10]. In previous works [11],several MMC with steel matrix were tested and there tribological behaviourwereprincipally affected by oxidation. Friction reduction and wear resistance significantly was enhanced by introduction of WS_2 in MMC's matrix.

The present study concerns five MMC containing solid lubricants trappedin a Stellite matrix. The interest of this MMC consist use of Stellite as the matrix. Yucel et al. [12] and Inman et al. [13] show that Stellite presents good tribological properties at high temperature. During tribological tests, this alloy produces oxides film with Co_3O_4 and $CoCr_2O_4$ and form a "glazed layer" that enhanced wear resistance.The production of Stellite matrix composite with solid lubricant would enhance friction reduction properties. In the present work, mechanisms responsible for the tribological behavior are identified and discussed. This approach is completed by surface topography measurements, observations of the third body morphology and chemical analyses of detached particles that compose the third body.

Materials studied

Metal Matrix Composites were synthesized under uniaxial pressure using a powder consolidation technology called Spark Plasma Sintering [14, 15]. The temperature of densification proceeds from current pulses of very high intensity, which directly pass through graphite dies and disperse spark plasma energy between particles of powder. This operation takes only a few minutes. The apparatus performed for this study is a Sumitomo Model 2080 located at the PlateformeNationale de Frittage Flash (PNF^2-CNRS) in Toulouse, France [16]. This is one of the most powerful machines in Europe in terms of current pulses (1-8000 A under 0-10 V) and sample size (up to 50 mm in diameter). Applied uniaxial pressure and sintering temperature can reach respectively 200 MPa and 2000°C.

The matrix of these composites is made of Stellite 6 containing about 30% in chromium, and 5% in tungsten (by weight). Table 1 presents the average chemical composition of the initial Stellite 6 according to ref 17.This alloy, without solid lubricant, so called Stellite, was chosen as a reference for the study.

Table 1: Chemical composition of Stellite 6 [17]

Element	Co	Cr	W	Fe	C	Mn	Si
% by weight	Matrix	27-32	4-6	2.5	0.9-1.4	1.0	1.0

Different amounts of hexagonal boron nitride (h-BN) or tungsten disulphide (WS_2) solid lubricants are introduced into the matrix. Table 2presents the sintering conditions of the six studied materials and their designation used in this paper.SPS conditions are optimized to obtain the best compaction of the material. In this way, the SPS conditions for A10BN are different in comparison to the others. The hardness measurement is presented to complete the mechanical characterization. Hardness increases with the amount of WS_2 and decreases with the amount of h-BN.

Table 2:Compositions and sintering conditions of the different studied MMC.

Materials	SPS Conditions	Hardness HV	Nomenclature
Stellite 6	900°C, 2 min, 80 MPa	452±2	Stellite
Stellite – 10% (vol.) h-BN	1000°C, 2 min, 80 MPa	380±20	St10BN
Stellite – 15% (vol.) h-BN	1000°C, 2 min, 80 MPa	300±30	St15BN
Stellite – 5% (vol.) WS_2	1000°C, 10 min, 100 MPa	537±6	St5WS_2
Stellite – 10% (vol.) WS_2	1000°C, 2 min, 80 MPa	541±8	St10WS_2
Stellite – 20% (vol.) WS_2	1000°C, 2 min, 80 MPa	570±20	St20WS_2

Experimental details

Tribological tests were performed using a Pin-on-disc configuration[18, 19].All pins are stainless steel AISI 431, and have a cylindrical shape of 6 mm diameter. Vickers hardness of the pins is 247 HV_{30}.Discs and pins were polished and cleaned in ultrasonic baths of ethanol prior testing.Tests are performed at a constant load of 15 N while the velocity increases by steps from 0.25 m/s to 1.5 m/s. Each steps has duration of 300 s.The normal load applied on the pin and tangential force arecontinuously measured throughout a computerized data acquisition system. The friction coefficient, also noted μ, is calculated according to the Amontons'law [20], *i.e.* the ratio of tangential force and normal load,while the wear rate is quantified using the Archard model [21].

Samples are heated up to 450°C by a radiative furnace surrounding the contact and thermocouples control the temperature in the vicinity of the contact. All tests are performed in air at atmospheric pressure. Table 3summarizes the operating conditions.

Table 3: Operating conditions of the tribometer.

Configuration	Plate on plate
Type ofmovement	Continues rotation
Pin diameter	6 mm
Contact area	113 mm^2
Temperature	450°C
Environment	Air – atmospheric pressure

Study of friction-reducing properties

Characteristic friction coefficient curves are represented as a function of time and the normal load for each composite in Figure 1to Figure 4. The friction coefficient valuesare presented in the text as an average for each step. A general evolution of the frictional properties is proposed.The vertical line that appears at each step beginning is an artifact of the acquisition system due to the introduction of the additional normal load.

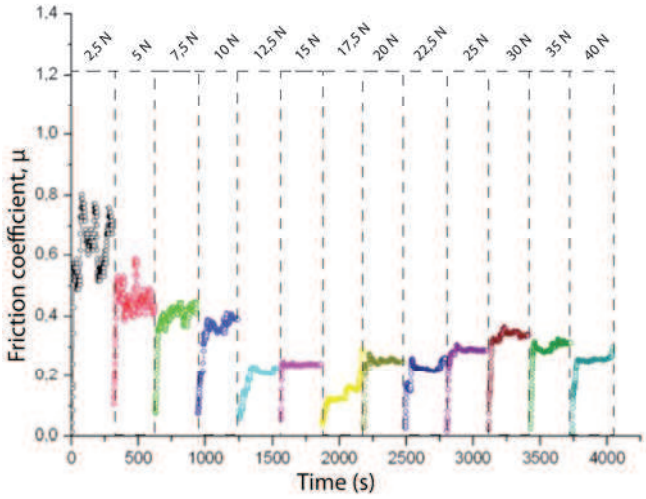

Figure 1: Friction coefficient of Stellite with respect to the time and normal load.

In the case of Stellite (Figure 1),the friction coefficient start at 0.63, it evolution during the two first steps is irregular. With increase of the normal load, friction coefficient decreases. The lowest value, 0.13, is obtained at 17.5 N. Note that after 5 N, the friction coefficient is very stable. After this step, the friction coefficient increases to values include between 0.25 and 0.33. This test is considered as a reference for the next tribological tests.

Tribological tests carried out with composites containing 10% by vol. of hexagonal boron nitride,*i.e.*St10BN (Fig.2 a),register average friction coefficients around 0.53 at the first step. The friction coefficient progressively decreases to 0.35.

In the case of St15BN (Fig.2 b), the friction coefficient follows globally the same evolution than St10BN. The values of μ are high at the test start and decrease step by step, from 0.85 to 0.46. The frictional force oscillates during the entire test and those oscillations are stronger at the three last stepswhere the friction coefficient associated is measured between 0.7 and 0.3.

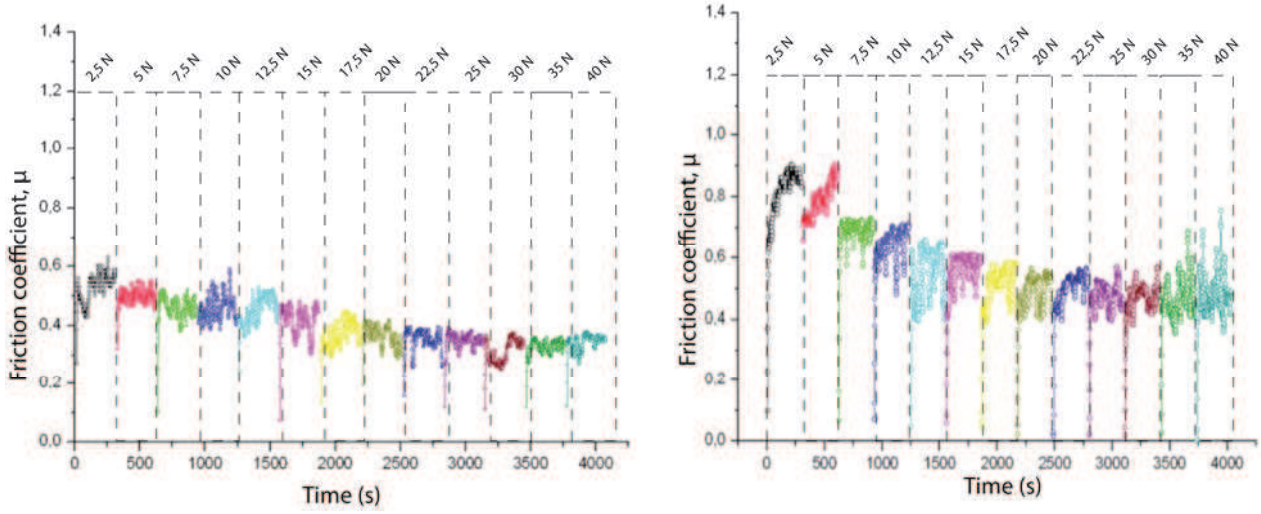

(a) (b)

Figure 2: Friction coefficient of St10BN (a) and St15BN (b) with respect to the time and normal load.

TheFigure 3(a) presents the friction coefficient recordedof $St5WS_2$ compositeis relatively stable in comparison with MMC containing h-BN. The highest values (μ=0,5) are measured during the first step and μ averaged 0.3 after applying a normal load of 17.5 N.

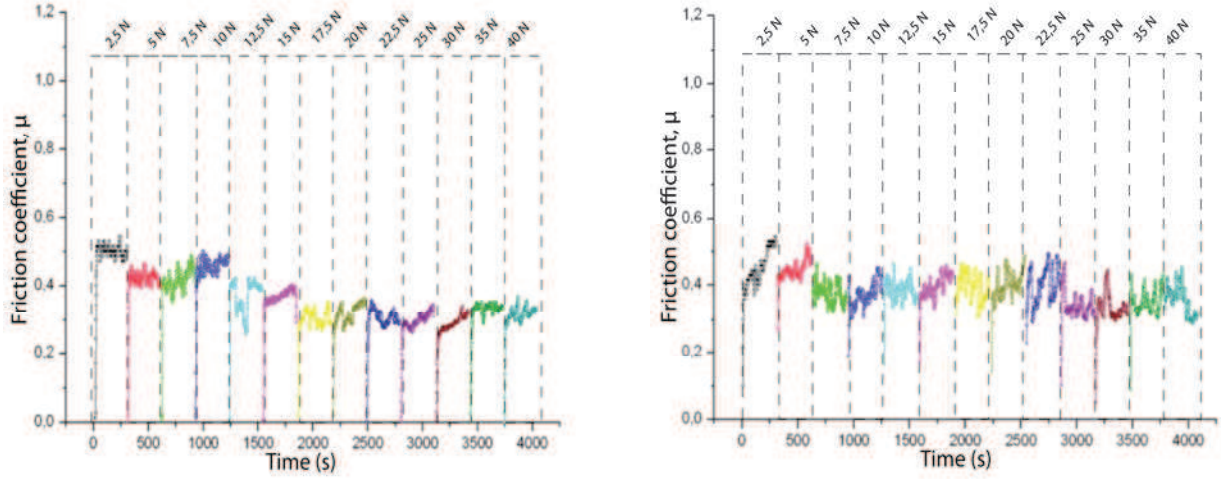

(a) (b)

Figure 3: Friction coefficient of $St5WS_2$ (a) and $St10WS_2$ (b) with respect to the time and normal load.

With St10WS_2(Figure 3(b)), the friction coefficient is starting around 0.4 and increase quickly to 0.5. During the test, the friction coefficient is irregular. With the increase of the normal load the friction coefficient oscillated around a mean value of 0.4. The maximum μ is evaluated at 0.54 and the minimum at 0.3

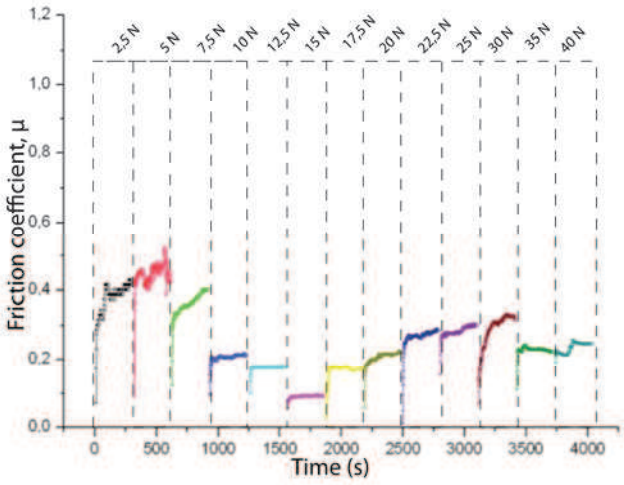

Figure 4: Friction coefficient of St20WS_2 with respect to the time and normal load.

The last compound, St20WS_2, presents in Figure 4 a behavior similar to that of the Stellite: for low load, between 2.5 and 5 N, the friction coefficient increases from 0.3 to 0.5. Then μ decrease with the normal load and is very stable. No oscillation is produced during the registration of μ, and each step corresponds to a very stable situation. Step by step, the friction coefficient reaches successivelythe values of 0.21, 0.16 and 0.09 respectively for the charge step of 10, 12.5 and 15 N. After 15 N, μ increases gradually to 0.17 at 17.5 N, 0.21at 20 N, 0.27at 22.5 N, 0.28at 25 N and 0.3at 30 N. After 30 N, a new decrease of μ is recorded; the value maintains an average around 0.23.

Thus, the addition of WS_2 is more beneficial than the addition of h-BN. Large amounts of solid lubricant are required to access tribological performances comparable to Stellite ones.

Optical and topographical analysis of the worn surfaces

Optical microscope observations are realized before tribological tests(Figure 5). In the St10BN and St15BN samples, the micrographs indicate the presence of agglomerated solid lubricant in the Stellite matrix. These particles are absents from the micrographs of the Stellite without solid lubricant. Only little scars appear on the surface, they are associated to the preparation of the sample.

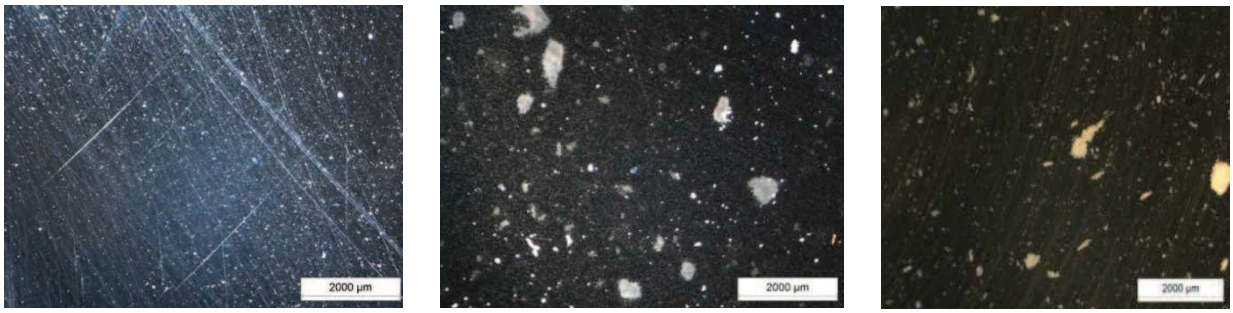

(a) (b) (c)

Figure 5: Optical micrographs of initial surfaces of (a) stellite, (b) St10BN and (c) St15BN.

Similar agglomerations of solid lubricant can be distinguished on the micrographs obtained with $St5WS_2$, $St10WS_2$ and $St20WS_2$ (Figure 6). The presence at the surface of the sample is expected to produce solid lubricant in the contact during the sliding motion of the pin on the disc.

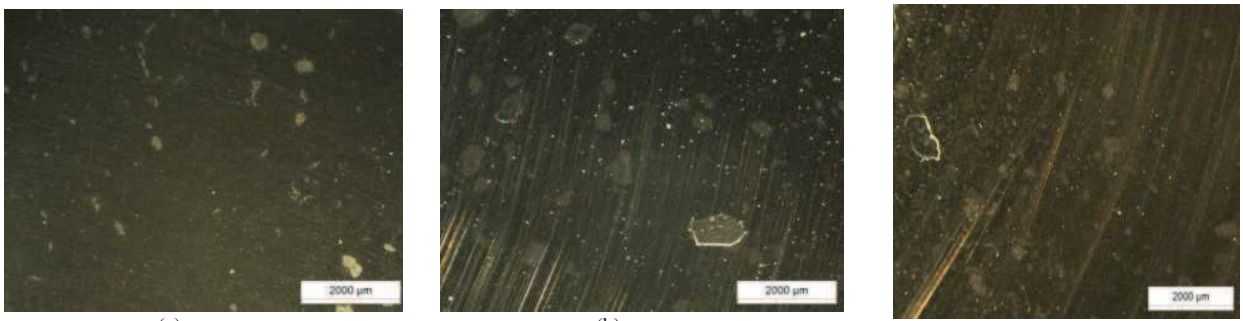

(a) (b) (c)

Figure 6: Optical micrographs of initial surfaces of (a) $St5WS_2$, (b) $St10WS_2$ and (c) $St20WS_2$.

Sliding surfaces were observed on both samples and sliders using an optical microscope (Figure 7 to Figure 12). All of the samples show evidences of abrasion and adhesive transfers of material inside the scar track. On Stellite sample, reddish and black debris adhere on the two contacting bodies (Figure 7). Numerous deformation scratches can also be distinguished on all the observed surfaces.

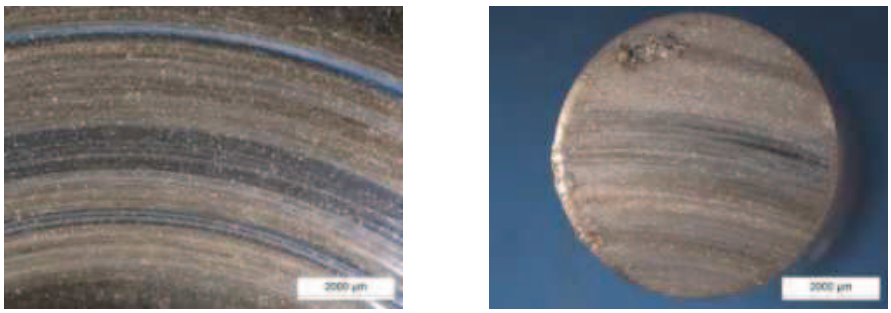

(a) (b)

Figure 7: Binocular microscopy images (a) of the Stellite sample (b) and of the pin.

Composites containing h-BN are also affected by an important degradation (Figure 7 and Figure 8). Fine particles can be collected near thescar of the discs. Black and grey particles are sprayed and stuck on both contacting surface. Numerous scratches can be observed on discs and pins.

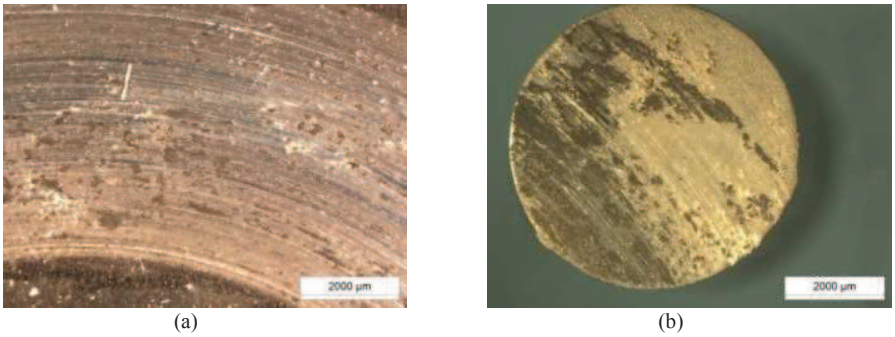

(a) (b)

Figure 8: Binocular microscopy images (a) of St10BN sample (b) and of the pin.

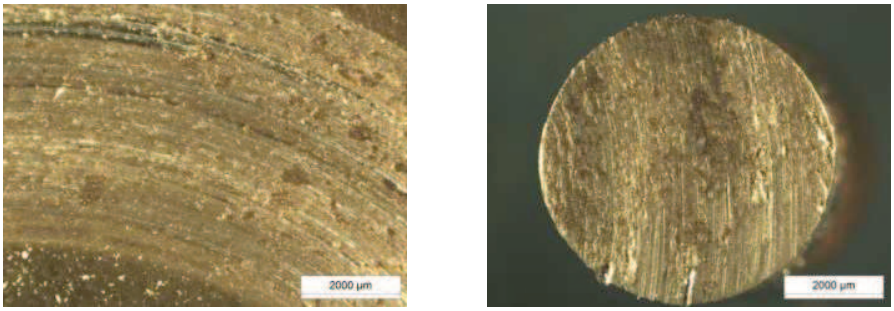

(a) (b)

Figure 9: Binocular microscopy images (a) of St15BN sample (b) and of the pin.

Samples containing WS_2 present a similar aspect to that observed on Stellite samples (Figure 10andFigure 12). Black particles are present on pins and discs, which form a highly shearing transfer layer crossing by numerous scratches. A black powder can be collected on the border of the scar at the end of the test.

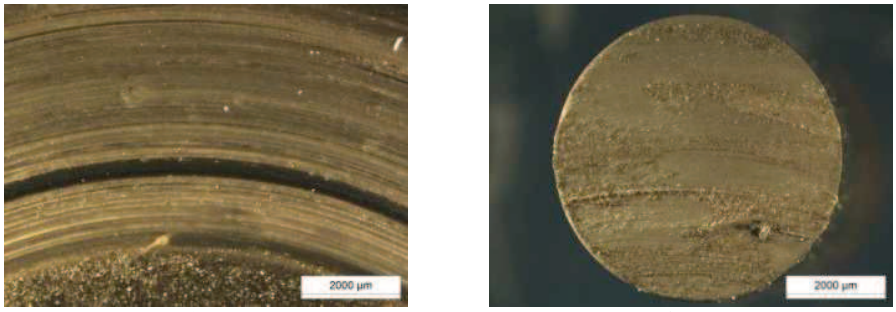

(a) (b)

Figure 10: Binocular microscopy images (a) of the $St5WS_2$ sample (b) and of the pin.

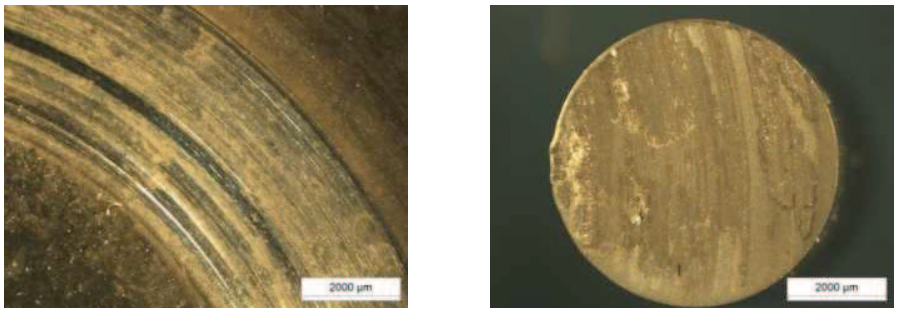

(a) (b)

Figure 11: Binocular microscopy images (a) of the $St10WS_2$ sample (b) and of the pin.

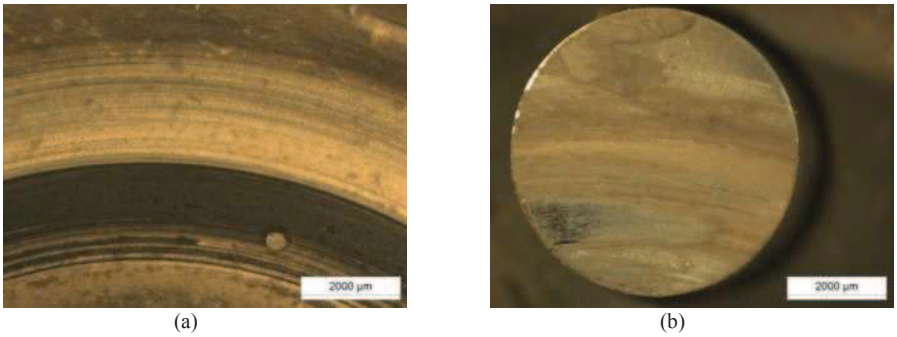

(a) (b)

Figure 12: Binocular microscopy images (a) of the $St20WS_2$ sample (b) and of the pin.

Topographic measurements are performed on a VYCO NT 1100 optical profiling system. Before tribological tests, pins show arithmetic roughness (R_a) of about 0.14 µm. Disc roughness is dependent on the material composition. Arithmetic roughness is ranged from 0.04 µm for the Stellite disc to 0.20 µm for the Stellite composite at 15% h-BN.

Table 4: Arithmetic and rms roughness values recorded before and after the tribological tests.

Material	Before the test		After the test	
	R_a [µm]	R_q [µm]	R_a [µm]	R_q [µm]
Stellite	0.04	0.06	3.08	3.54
Co10BN	0.15	0.33	3,44	4,42
Co15BN	0.20	0.43	8,12	10,14
$Co5WS_2$	0.09	0.13	2,78	3,92
$Co10WS_2$	0.13	0.17	3,80	4,91
$Co20WS_2$	0.08	0.12	2,17	4,90

Table 4 summarizes the arithmetic roughness and rms roughness (R_q) for the sliding pin and the six composites of this study.MMC arithmetic roughness is generally higher than these of the Stellite disc. Thus, the polishing preparation led to a relatively smooth surface on Stellite, while composites exhibit more irregular surfaces.Surfaces topography of Stellite and MMC, show that the roughness parameters are increased after tribological tests for overall studied samples (Table 4).

On Stellite disc, the three-dimensional images reveals well marked scratches alternated with very flat planes. This aspect is associated to the abrasion of the disc during the test (Figure 13). The corresponding measured arithmetic roughness R_a reaches 3.08 µm.

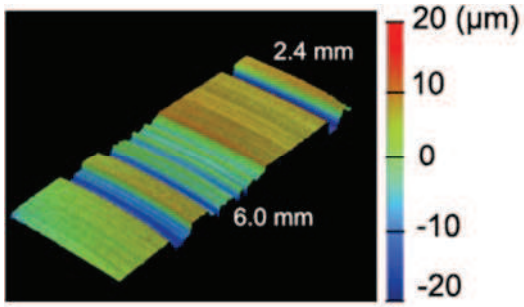

Figure 13:Three-dimensional image of Stellite recorded by optical profilometry.

Figure 14 (a) and (b) were recorded on the worn surfaces of samples containing h-BN. The powder particles remain present at the surface of these samples. Roughness parameters are measured: R_a = 3.14 µm for St10BN, this is the same scale than Stellite.For St15BN,R_a = 8.12 µm, it is higher than the values measured for Stellite. Thus, after the friction test the MMC that contains the highest amount of h-BN present important degradation in comparison of the Stellite without lubricant.

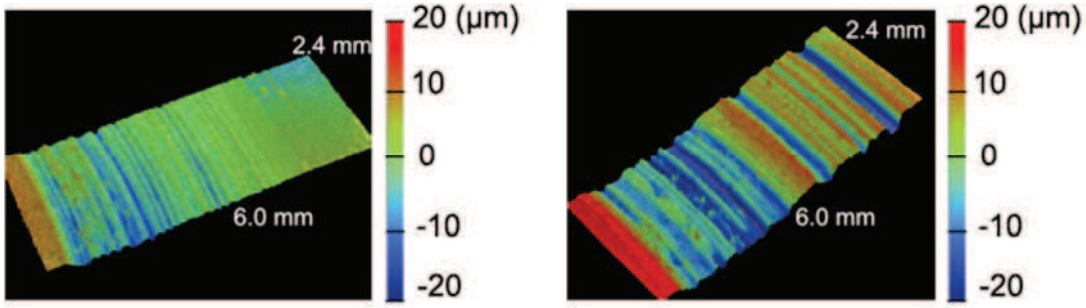

(a) (b)

Figure 14: Three-dimensional images of St10BN (a) and St15BN (b) recorded by optical profilometry.

For the discsproduce with St5WS2 (Figure 15 (a)), the average roughness parameter is lower than in the case of the pristine Stellite, R_a=2.78 µm. Scratches can be observed but most of the surface is flat. This is also the case for the samples that contain 10% of WS_2 (Figure 15(b)). Nevertheless, R_a is higher and equal 3.80 µm. For these two samples,scratches are less deep and surfaces show a smoother pattern. A general deformation of the last disc, made with St20WS2, is evidenced. Thus, the arithmetic roughness R_a is lowestmeasured of all experiments. No scar appears on the 3D topographic map (Figure 15 (b)). But the value of the root mean square roughness is high: 4.90. This disc presents a global inelastic deformation. The dimension of this deformation is larger than the surface where the pin slid during the tribological tests.

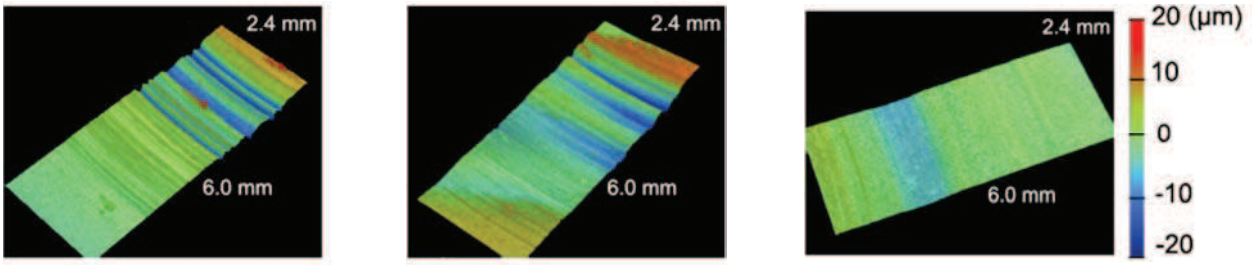

(a) (b) (c)

Figure 15: Three-dimensional images of $St5WS_2$(a), $St10WS_2$(b)and $St20WS_2$(c) recorded by profilometry.

Studies of wear and damage

The three-dimensional images of the sample damages allow a quantitative analysis of the missing volume V_- (volume below the reference plane defined by the initial undamaged surface) and the displaced volume V_+ (volume above the previous reference plane). The difference between these two volumes gives the wear volume $V_w$of the studied section. The total wear volume V_T is determined using the following expression, where r is the average radius of the wear track and l is the width of the analyzed section:

$$V_T = V_w \cdot \frac{2\pi r}{l} \quad (1)$$

Wear rate $U_w$is calculated from the previous total volume values by using the Archard model and assuming that wear is a linear function of covered distance. For the present tests, the wear rates are given by the following formula:

$$U = \frac{V_T}{L_T \cdot \Sigma_i F_{Ni}} \quad (2)$$

L_T is the total distance travelled during the test;F_{Ni} represents the successive normal loads applied to the samples during the i^{th} step. All values of wear rate for the different discs are given in Table 5.

Table 5: Wear rate of the studied materials.

Material	Wear rate of the disc $[\mu m^3 \cdot N^{-1} \cdot m^{-1}]$
Stellite	$-9{,}6 \cdot 10^1$
Co10BN	$-8{,}7 \cdot 10^1$
Co15BN	$-1{,}1 \cdot 10^2$
$Co5WS_2$	$-6{,}2 \cdot 10^1$
$Co10WS_2$	$-6{,}3 \cdot 10^1$
$Co20WS_2$	$-4{,}1 \cdot 10^1$

Wear rate all discs are negatives. A negative wear rate indicates that the transfer of material from the pin is greater than the loss of material in the disc. The highest wear ratesare calculated for Stellite and the MMC that contain h-BN. The lowest wear rate is measured for composites that contained WS2 solid lubricant. The endurance of the composites has been improved by the addition of this lubricant in the Stellite matrix.

Micromorphology analysis

Micrographs were performed on a Jeol JSM-7000F scanning electron microscope, equipped with a field effect electron gun. This device also allows the acquisition of secondary electrons images (SEI) and backscattered electrons images with a chemical contrast.Micrographs are recorded with 15 kV accelerated tension and a working distance of 10 mm. Three composites are chosen to perform the micrography: Stellite, St10BN and St10WS2.

The micrographs reveal the morphology of the disc worn surface.For Stellite disc(Figure 16 (a)), the SEIfiguresa surface marked with scratches, slip zoneand material agglomeration with shear zones.Figure 16 (b) shows the composition contrast on the surface. Two colors are distinguished: white and grey, these colors are respectively associated to cobalt and iron. Iron particle are transferred from the pin to the disc surface. This transfer is due to the relatively low hardness of the pin with respect to the disc the disc.

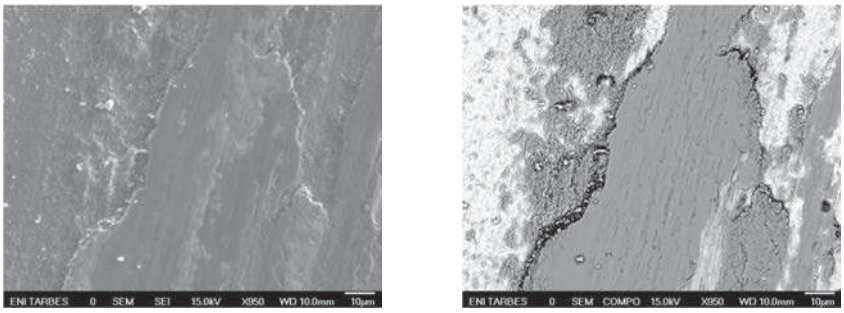

(a) (b)

Figure 16: Observations by SEM of the Stellite sample with two different observation modes: secondary electron and backscattered electron with chemical contrast.

The surface of the MMC containing h-BN solid lubricant, St10BN,reveals platelet andpowdery particles (Figure 17).Grains appear near holes and seem to be ready to be extracted from the composite surface. The micrograph with chemical contrast (Figure 17 (b)) presents 3 colors: white, for the cobalt, grey, for iron, and black, for the solid lubricant, h-BN. The lubricant is located in holes and between the Stellite grains. The lubricant is extracted and mixed to metal particles and contributed to the formation of a third body.

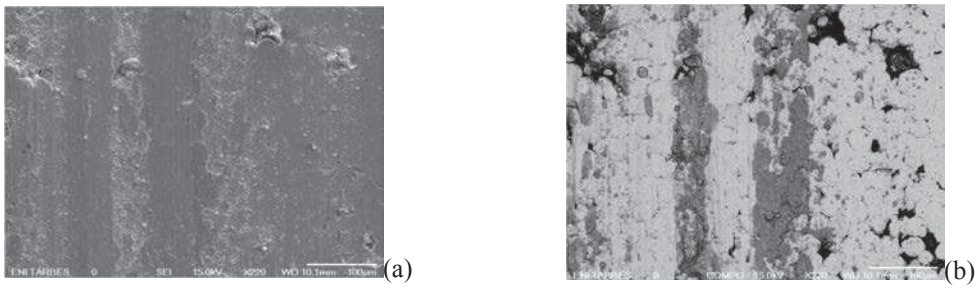

Figure 17: Observations by SEM of theSt10BN with two different magnificationsobservation modes: secondary electron and backscattered electron with chemical contrast.

Finally, the surface imagesfrom the composite surface containing WS_2 ($St10WS_2$) looks like tribofilms from Stellite, with compacted particles and layers of high sheared(Figure 18). Chemical image also shows the presence of iron (in grey) on the MMC (in light grey).

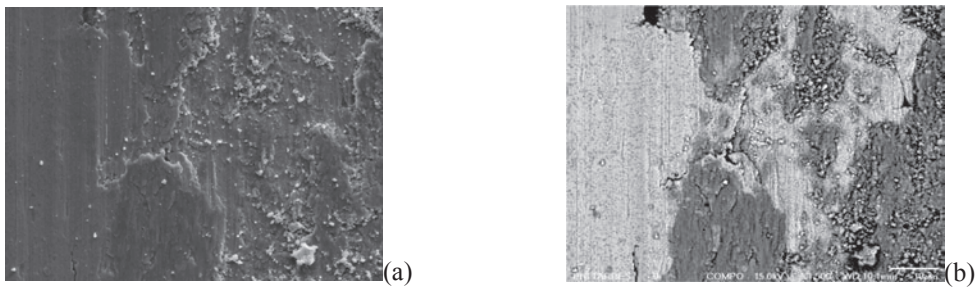

Figure 18: Observations by SEM of the sliding surface of the $St10WS_2$ with two different observation modes: secondary electron and backscattered electron with chemical contrast.

Discussion

The topographic, morphological, and chemical analyses revealed the formation of tribofilms during friction tests. The overall degradation mechanisms of all compounds studied involve both abrasive wear and adhesive wear associated to an oxidization process. These third bodies protect the surfaces of the pins and the discs by accommodating the shear stresses.Tribological films are produced by production of particles from both pins and discs. This third body mostly consistswithsteel, Stellite and solid lubricant, when it's available, but alsowith metal oxides coming from the pin and the disc surfaces, as shown previously by other authors.

Figure 19 represents the friction coefficient of MMC with h-BN and the Stellite. It clearly appears a degradation of the friction reduction properties by addition of this solid lubricant in the Stellite matrix. The greater the amount of h-BN, the higher the degradation is high. The deformation of the surface follows this tendency too as shown in the topographic analysis (Table 4). This degradation is observed also for the wear resistance (Table 5). Indeed, the compound that containing the largest amount of h-BN is the one with the highest wear rate.

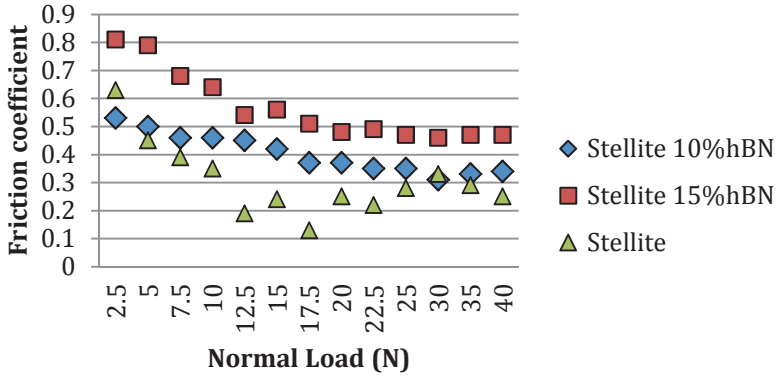

Figure 19: Friction coefficient versus the applied normal load for Stellite, and Stellite with 10% and 15% (vol.) of h-BN

These performances can be explained by the modification of the microstructure and the reduction of the hardness of the compound with the addition of h-BN (see Table 2). St10BN and St15BN emitted a lot of particles in comparison to Stellite. These particles are mixed with iron particles from the pin, and can be oxidized. It appears a third body that is not efficient to lowering the friction coefficient. A part of this third body is then ejected from the contact and produce wear particles. The third body can't stay in the contact to protect the surface of the two first bodies. This is probably due to the incapacity of h-BN to adhere to the surface of the pins and the discs.

The addition of WS_2 changes the tribologic properties of the composite. Wear rate is reduced, with respect to the hardness. Due to the presence of WS_2, the third body remains stable and more cohesive that enable it to protect the sliding surfaces efficiently by relaying the most part of the shear stresses. It contributes to adaptation of velocities between the two contacting bodies. The friction coefficient is also lowered in comparison to MMC that contains the biggest amount of h-BN. In St20WS2, an inelastic deformation is observed on the disc and participates to the adaptation of the two first bodies when the normal load is applied. By increasing the amount of WS_2, friction reduction properties are reinforced, and sometimes μ for MMC with highest amount of WS_2 is lower than in the case of Stellite.

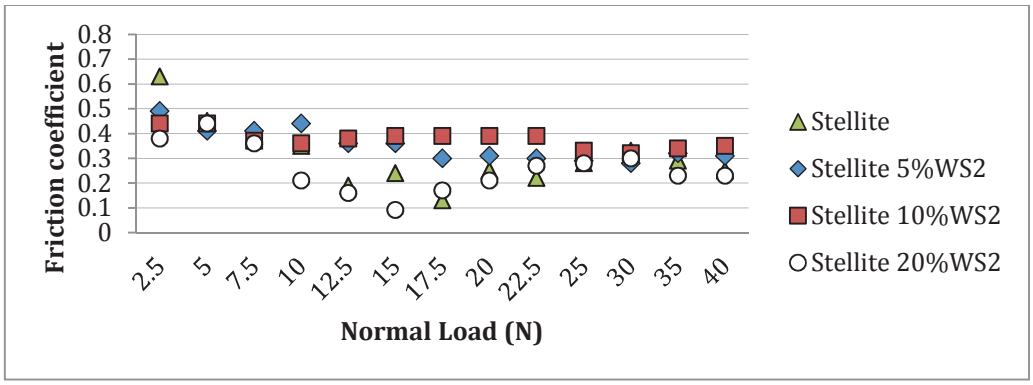

Figure 20:Friction coefficient versus the applied normal load for Stellite, and Stellite with 5%, 10% and 15% (vol.) of WS_2.

So, depending on the nature of the solid lubricant, two opposites effects are observed on the tribologicalperformances of the third body: degradation or improvement of the tribological properties.

Conclusion

In order to offer efficient materials for tribological applications at high temperature (450°C), metal matrix composites (Stellite matrix) including solid lubricant particles (different contents of h-BN or WS_2) were developed using a SPS technique of powder consolidation. Tests were carried out using a rotative Pin-on-disc tribometer at 450°C and under varying normal load at a constant velocity.

The third body concept is takes into account, and highlights the ambiguous role of h-BN and WS_2 introduced into the matrix on the friction and wear properties. The identified wear mechanisms essentially correspond to adhesive wear (transfer phenomenon) and abrasive wear (numerous scratches). In agreement to previous work, the occurrence of oxidization of the Stellite, Stellite matrix composite and iron contained in the pin, is supposed,but has to be certified by more precise chemical analysis. However, the choice of the Stellite permits to produce materials that are also able to protect the surfaceduring the friction conditions.Unlike h-BN, solid lubricant, such as WS_2, seems to be a good prospect to promote the formation of a stable tribofilm, able to take over the shearing stresses and ensure the velocity adaptation, necessary between the two first bodies.To withstand the severe working conditions, this third body acts as a relay.

Acknowledgements

The authors wish to thank the French Interregional action of Midi-Pyrénées and Aquitaine for its financial support, the PNF^2 platform and the CEMES of Toulouse for the synthesis and the development of optimized samples for this study.

References

[1] T. Childs,Tribology International, Vol. 13, (1980), p. 285

[2] Y. Watanabe : Contact Characteristics of New Self-Lubricating Composite Materials, (IEICE Trans. Electron., Japan1994).

[3] M. E. Fine,(1990),Recent Advances in Tribology, Northwestern Univ. ed., Y.C. Chung and H.S. Cheng, Eds., Evanston.

[4] Y. Pauleau, N. Marechal, P. Juliet, C. Zimmermann, and R. Gras,Lubrication Engineering, Vol. 52, (1996),p. 481.

[5] J. D. Bolton and A. J. Gant, Journal of MaterialProcessingTechnology, Vol. 56, (1996), p 136-147.

[6] B. Chen, Q. Bi, J. Yang, Y. Xia and J. Hao, Tribology International, Vol 41, (2008), p 1145-1152.

[7] W. Chen, Y. Gao, C. Chen, J. Xing, Wear, Vol 269, Issues 3-4, (2010), p 241-248.

[8] Y. Kimura, T. Wakabayashi, K. Okada, T. Wada and H. Nishikawa,Wear, Vol. 232, (1999), p. 199.

[9] Y. BerthierIn: Handbook of Materials Behavior Models, edited by J. Lemaître, Academic Press, (2001), p. 679

[10] J. Denape, Y. Berthier, and L. Vincent, In: Fundamentals of tribology and bridging the gap between the macro- and micro/nanoscales, edited by B. Bhushan, Kluwer Academic Publishers, (2001),p. 393

[11] S. Orozco Gomez, K. Delbé, A. Benitez, J.-Y. Paris, J. Denape Key Engineering Materials,Vol. 482, (2011), p. 89-100

[12] B. Yucel, Wear, Vol. 269 (2010), p 664-671

[13] I. A. Inman, S.R. Rose, P. K. Datta, Tribology international,Vol. 39, (2006) 1361-1375

[14] K. Inoue. U.S. Patent No. 3,241,956. (1966)

[15] R. Orru, R. Licheri, A. Mario Locci, A. Cincotti, G. Cao, Materials Science and Engineering : R, Vol. 63, (2009) p. 127.

[16] Information on http://pnf2.dr14.cnrs.fr/

[17] J.R. Davis, (2000), ASM Specialty Handbook: Nickel, Cobalt and Their Alloys, ASM international,

[18] A.S. Adamou, J. Denape, J.-Y. Paris, and E. Andrieu,Wear, Vol. 261, (2006), p. 311

[19] A. S. Adamou, Thesis, Institut National Polytechnique de Toulouse, (2005)

[20] G. Amontons,“Du frottement de diversesmatières les unescontre les autres” (1699)

[21] J. F. Archard, Journal of applied physics, Vol. 24, (1953), p. 981

Behaviour of Material and Composite Structures
10.4028/www.scientific.net/KEM.498

Tribological Behaviour of Stellite Matrix Composites for High Temperatures Applications
10.4028/www.scientific.net/KEM.498.89

DOI References
[5] J. D. Bolton and A. J. Gant, Journal of MaterialProcessingTechnology, Vol. 56, (1996), pp.136-147.
doi:10.1016/0924-0136(95)01829-8
[6] B. Chen, Q. Bi, J. Yang, Y. Xia and J. Hao, Tribology International, Vol 41, (2008), pp.1145-1152.
doi:10.1016/j.triboint.2008.02.014
[7] W. Chen, Y. Gao, C. Chen, J. Xing, Wear, Vol 269, Issues 3-4, (2010), pp.241-248.
doi:10.1016/j.wear.2010.04.003
[8] Y. Kimura, T. Wakabayashi, K. Okada, T. Wada and H. Nishikawa, Wear, Vol. 232, (1999), p.199.
doi:10.1016/S0043-1648(99)00146-5
[11] S. Orozco Gomez, K. Delbé, A. Benitez, J. -Y. Paris, J. Denape Key Engineering Materials, Vol. 482, (2011), pp.89-100.
doi:10.4028/www.scientific.net/KEM.482.89
[12] B. Yucel, Wear, Vol. 269 (2010), pp.664-671.
doi:10.1016/S0167-5273(10)70156-X
[13] I. A. Inman, S.R. Rose, P. K. Datta, Tribology international, Vol. 39, (2006) 1361-1375.
doi:10.1016/j.triboint.2005.12.001
[18] A.S. Adamou, J. Denape, J. -Y. Paris, and E. Andrieu, Wear, Vol. 261, (2006), p.311.
doi:10.1016/j.wear.2005.11.008
[21] J. F. Archard, Journal of applied physics, Vol. 24, (1953), p.981.
doi:10.1063/1.1721448